

Supplementary information

Enhancement of the output voltage of droplet electricity generators using high dielectric high-entropy oxide composites

Yanan Zhou^{a,c#}, Yan Zeng^{a#}, Jianming Wang^{a,b#}, Xiaoyi Li^d, Peng Wang^{a,c*}, Wenlong Ma^a, Congyu Wang^{a,c}, Jiawei Li^a, Wenyong jiang^a, Dun Zhang^{a,c}

^a Key Laboratory of Marine Environmental Corrosion and Bio-fouling, Institute of Oceanology, Chinese Academy of Sciences, Qingdao 266071, China

^b Institute of Marine Corrosion Protection, Guangxi Key Laboratory of Marine Environmental Science, Guangxi Academy of Marine Sciences, Guangxi Academy of Sciences, Nanning.530007, China

^c University of Chinese Academy of Science, Beijing 100049, China

^d College of Materials Science and Engineering Ocean University of China Qingdao 266100, China

* Corresponding author: Key Laboratory of Marine Environmental Corrosion and Bio-fouling, Institute of Oceanology, Chinese Academy of Sciences, Qingdao 266071, China. E-mail: wangpeng@qdio.ac.cn

These authors contributed equally to this work

Part 1: Supplementary Note S1 determination of lattice constant

Part 2: Table S1 Sequences of oligonucleotides used in the work

Part 3: Table S2 Comparison table among traditional electrochemical methods for DNA detection and this work

Part 4: Fig. S1 Equivalent circuit diagram of the droplet falling process.

Part 5: Fig. S2 Current output of HP-DEG with different intermediate layer thicknesses.

Part 6: Fig. S3 Current output of HP-DEG with different falling heights.

Part 7: Fig. S4 Current output of HP-DEG with different friction layer angles.

Part 8: Fig. S5 Current output of HP-DEG at different mass concentrations of HEOs@PDMS.

Part 9: Fig. S6 Current output of DEG with other organic materials as intermediate layer. (Blank, PDMS, PDMS@HEOs, PTFE, PI)

Part 10: Fig. S7 Dielectric constants and voltages comparative plots of DEG with various materials used as intermediate layer.

Part 11: Fig. S8 Voltage output of DEG and HP-DEG with different load resistances.

Part 12: Fig. S9 Voltage output of DEG, HP-DEG by charging 47/100 μ F capacitors.

Part 13: Fig. S10 FTIR spectroscopy of Fe_3O_4 , amido- Fe_3O_4 , amido- Fe_3O_4 modified on capture probe.

Part 14: Fig. S11 Voltage output of HP-DEG for bacterial DNA sensing with different reaction times for DNA complex formation (30, 60, 90, 120, 150 min).

Part 15: Fig. S12 Voltage output of DEG with different dilutions of CNTs. After taking 10 ml of the original solution, the dilutions were 10^1 , 10^2 , 10^3 , 10^4 , 10^5 respectively.

Part 16: Fig. S13 Voltage output of HP-DEG with different dilutions of CNTs. After taking 10 ml of the original solution, the dilutions were 10^1 , 10^2 , 10^3 , 10^4 , 10^5 respectively.

Part 17: Fig. S14 DNA gel electrophoresis graph. (a) 20bp marker (b) DNA (c) Capture probe (d) Signal probe (e) Capture probe+DNA (f) Capture probe+DNA+Signal probe

Part 18: Fig. S15 Standard curve of DEG based bacterial DNA sensing.

Part 19: Fig. S16 Standard curve of HP-DEG based bacterial DNA sensing.

Part 20: Fig. S17 HP-DEG based bacterial DNA sensing platform. a) 3D printed platform b) Physical specimen image.

Part 1: Supplementary Note S1: determination of lattice constant

(FeNiCrMn)₃O₄ HEO

HRTEM:

1. d-spacing for the crystalline plane (311) of (FeNiCrMn)₃O₄ HEO: 0.2496 (nm). Take (*h k l*) to be (311),

$$d = \frac{a}{\sqrt{h^2 + k^2 + l^2}} \rightarrow a = d \times \sqrt{h^2 + k^2 + l^2} = 0.2496 \times \sqrt{3^2 + 1^2 + 1^2} = 0.82$$

2. d-spacing for the crystalline plane (400) of (FeNiCrMn)₃O₄ HEO: 0.2078 (nm). Take (*h k l*) to be (400),

$$d = \frac{a}{\sqrt{h^2 + k^2 + l^2}} \rightarrow a = d \times \sqrt{h^2 + k^2 + l^2} = 0.2078 \times \sqrt{4^2 + 0^2 + 0^2} = 0.83$$

XRD:

Bragg's law

$$\text{Bragg's law: } n\lambda = 2d\sin\theta$$

1. Diffraction peak (311): $2\theta = 35.70^\circ$, $\lambda = 0.154$ (nm),

$$d = \frac{1 \times 0.154}{2 \times \sin\left(\frac{35.70^\circ}{2}\right)} = 0.2512$$

$$d = \frac{a}{\sqrt{h^2 + k^2 + l^2}} \rightarrow a = d \times \sqrt{h^2 + k^2 + l^2} = 0.2512 \times \sqrt{3^2 + 1^2 + 1^2} = 0.83$$

2. Diffraction peak (400): $2\theta = 43.40^\circ$, $\lambda = 0.154$ (nm),

$$d = \frac{1 \times 0.154}{2 \times \sin\left(\frac{43.40^\circ}{2}\right)} = 0.2083$$

$$d = \frac{a}{\sqrt{h^2 + k^2 + l^2}} \rightarrow a = d \times \sqrt{h^2 + k^2 + l^2} = 0.2083 \times \sqrt{4^2 + 0^2 + 0^2} = 0.83$$

(FeNiCrMnCo)₃O₄ HEO

HRTEM:

1. d-spacing for the crystalline plane (311) of (FeNiCrMnCo)₃O₄ HEO: 0.2512 (nm).

Take (h k l) to be (311),

$$d = \frac{a}{\sqrt{h^2 + k^2 + l^2}} \rightarrow a = d \times \sqrt{h^2 + k^2 + l^2} = 0.2512 \times \sqrt{3^2 + 1^2 + 1^2} = 0.833$$

2. d-spacing for the crystalline plane (400) of (FeNiCrMn)₃O₄ HEO: 0.2084 (nm). Take

(h k l) to be (400),

$$d = \frac{a}{\sqrt{h^2 + k^2 + l^2}} \rightarrow a = d \times \sqrt{h^2 + k^2 + l^2} = 0.2084 \times \sqrt{4^2 + 0^2 + 0^2} = 0.833$$

XRD:

Bragg's law

Bragg's law: $n\lambda = 2d\sin\theta$

Diffraction peak (311): $2\theta = 35.64^\circ$, $\lambda = 0.154$ (nm),

$$d = \frac{1 \times 0.154}{2 \times \sin\left(\frac{35.64^\circ}{2}\right)} = 0.2516$$

$$d = \frac{a}{\sqrt{h^2 + k^2 + l^2}} \rightarrow a = d \times \sqrt{h^2 + k^2 + l^2} = 0.2516 \times \sqrt{3^2 + 1^2 + 1^2} = 0.833$$

2. Diffraction peak (400): $2\theta = 43.30^\circ$, $\lambda = 0.154$ (nm),

$$d = \frac{1 \times 0.154}{2 \times \sin\left(\frac{43.30^\circ}{2}\right)} = 0.2087$$

$$d = \frac{a}{\sqrt{h^2 + k^2 + l^2}} \rightarrow a = d \times \sqrt{h^2 + k^2 + l^2} = 0.2087 \times \sqrt{4^2 + 0^2 + 0^2} = 0.833$$

Part 2:

Table S1 Sequences of oligonucleotides used in the work

Primer	Sequences (5'to3')
Target DNA(SRB)	CGGCGTCGCTGCGTCAGG
Signal probe	GCGACGCCGTTTTTT-NH ₂
Capture probe	HOOC-TTTTTTCCTGACGCA
Three-mismatched bases	GGGCGTCGATGCGTCAGT
Single-mismatched base	CGGCGTCGATGCGTCAGG
DSV-687	TAC GGA TTT CAC TCC T
DSV-321	TGG GCC GTG TTT CAG T

Part 3:

Table S2 Comparison table among traditional electrochemical methods for DNA detection and this work

Target	Analytical methods	Core materials	Linear range	Detection volume	Device Portability	References
5hmC-DNA	electrochemical	Ti ₃ C ₂ T _x MXene materials	1.0 × 10 ⁻¹³ -1.0 × 10 ⁻⁹ M	-	No	[1]
cancer-derived exosomes	electrochemical	entropy-driven autocatalytic DNA circuit (EADC)	79 - 3.15 × 10 ⁵ particles/μL	-	No	[2]
miRNA-let-7a	electrochemical /colorimetric dual-mode	3D DNA Walkers and self-power	1.0 × 10 ⁻¹⁶ -1.0 × 10 ⁻⁸ M	1mL	Yes	[3]
microRNA	electrochemical	Double-response 3D DNA nanomachine	5.0 × 10 ⁻¹⁶ -1.0 × 10 ⁻¹¹ M	-	No	[4]
antibiotics	electrochemical	DNA tetrahe-	1.0 × 10 ⁻	-	No	[5]

		dron based	$9-1.0 \times 10^{-6}$ M			
		diblock	10^{-6} M			
		aptamer				
		immobilized				
DNA(SRB-385)	Single droplet electricity generators (SDEG)	HEOs@PDM S as an intermediate layer	1.0×10^{-6} M	50 μ L	Yes	This work

Part 4:

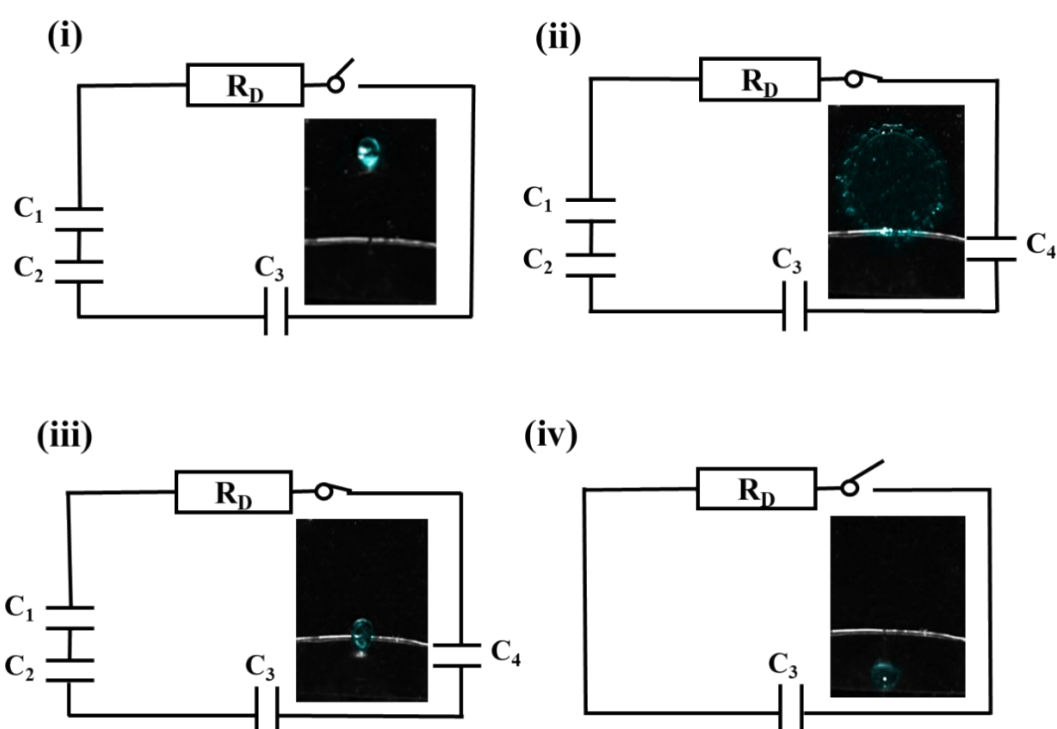


Fig. S1 Equivalent circuit diagram of the droplet falling process. (i) The droplet just falls onto the surface of the FEP film, (ii) State of the droplet spreading out on the surface of the FEP film and contacting the top electrode, (iii) The droplet gradually contracts on the FEP surface, resulting in a decrease in the contact area between the droplet and FEP as well as between the droplet and copper electrode. (iv) Droplets shrink and leave the FEP film.

Part 5:

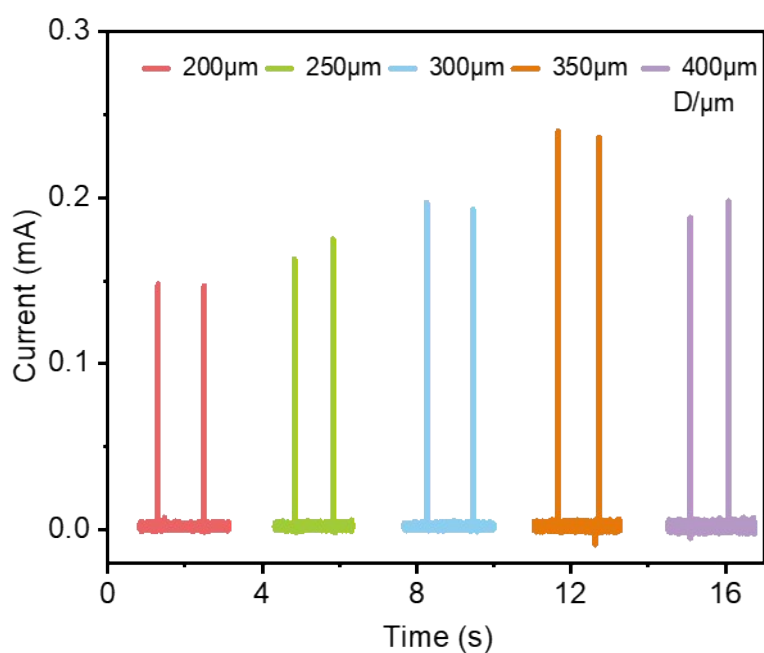


Fig. S2 Current output of HP-DEG with different intermediate layer thicknesses.

Part 6:

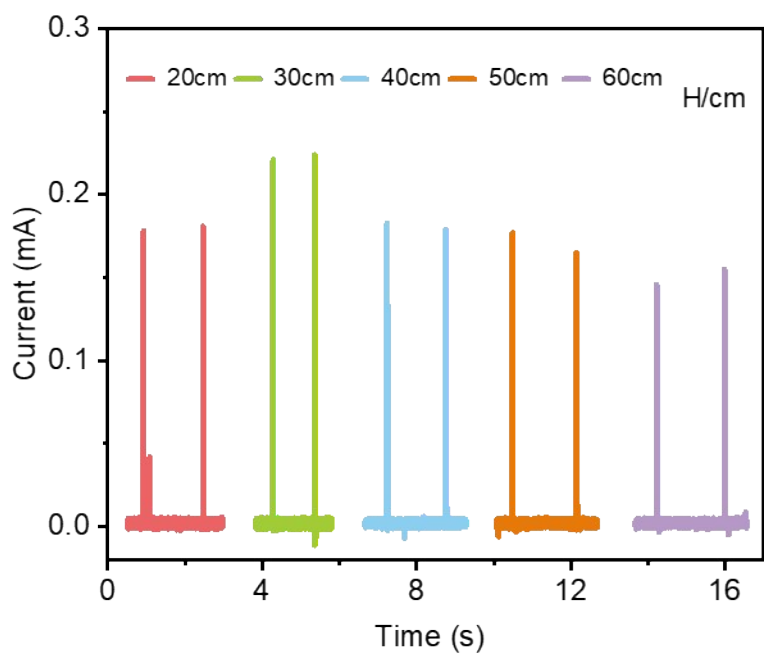


Fig. S3 Current output of HP-DEG with different falling heights.

Part 7:

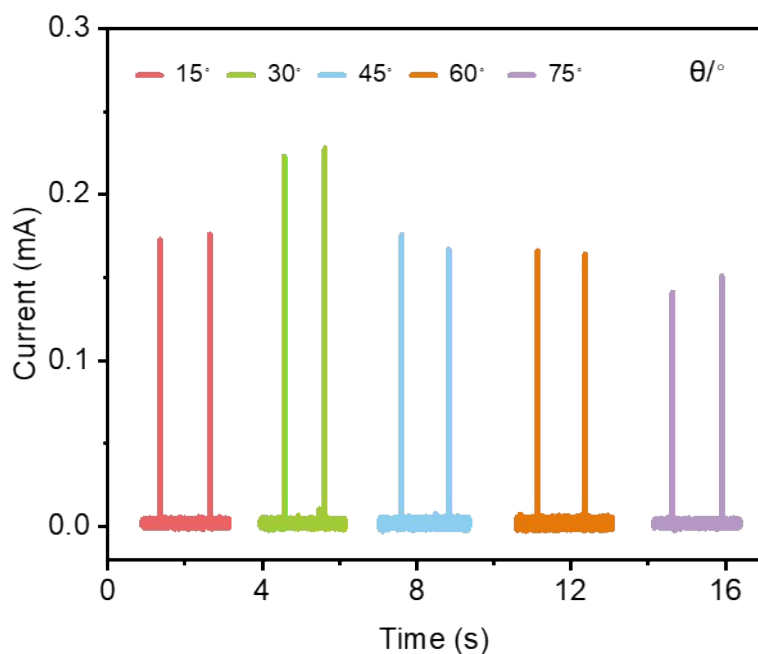


Fig. S4 Current output of HP-DEG with different friction layer angles.

Part 8:

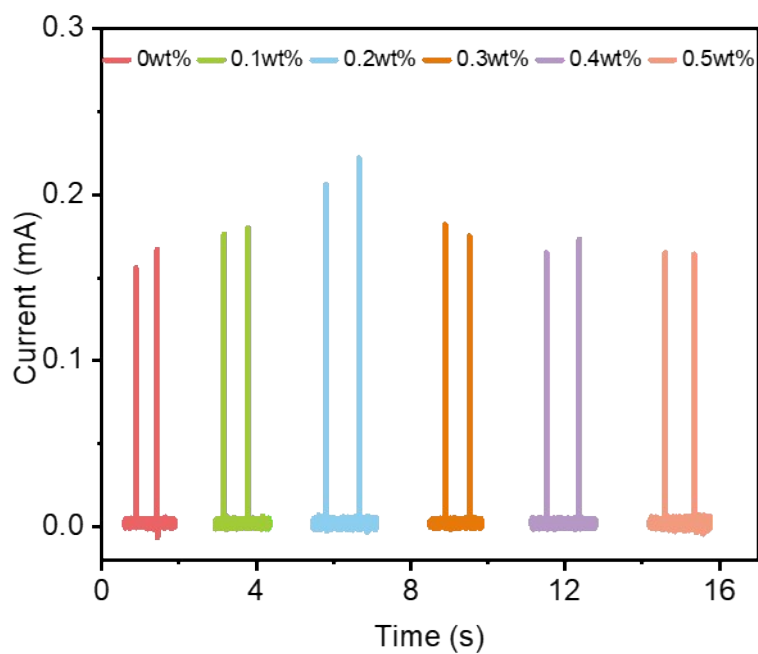


Fig. S5 Current output of HP-DEG at different mass concentrations of HEOs@PDMS.

Part 9:

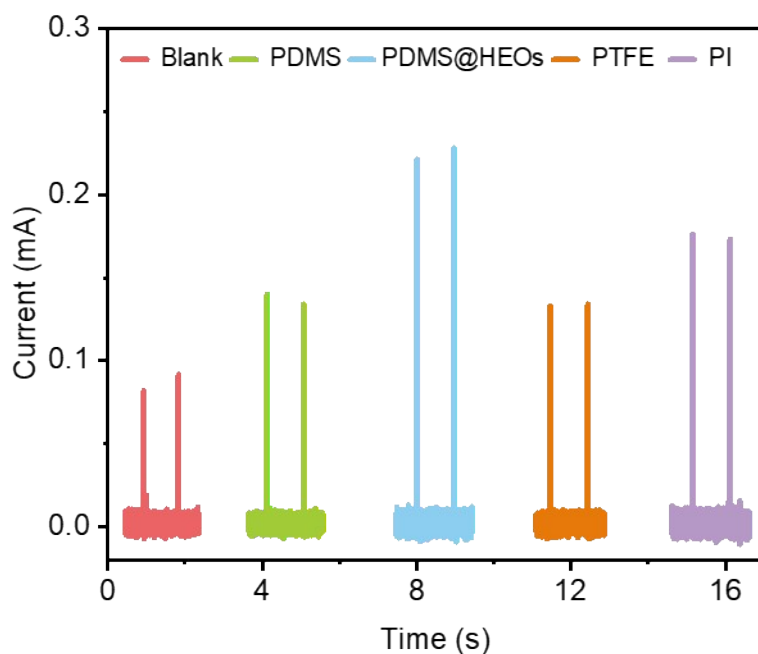


Fig. S6 Current output of DEG with other organic materials as intermediate layer. (Blank, PDMS, PDMS@HEOs, PTFE, PI)

Part 10:

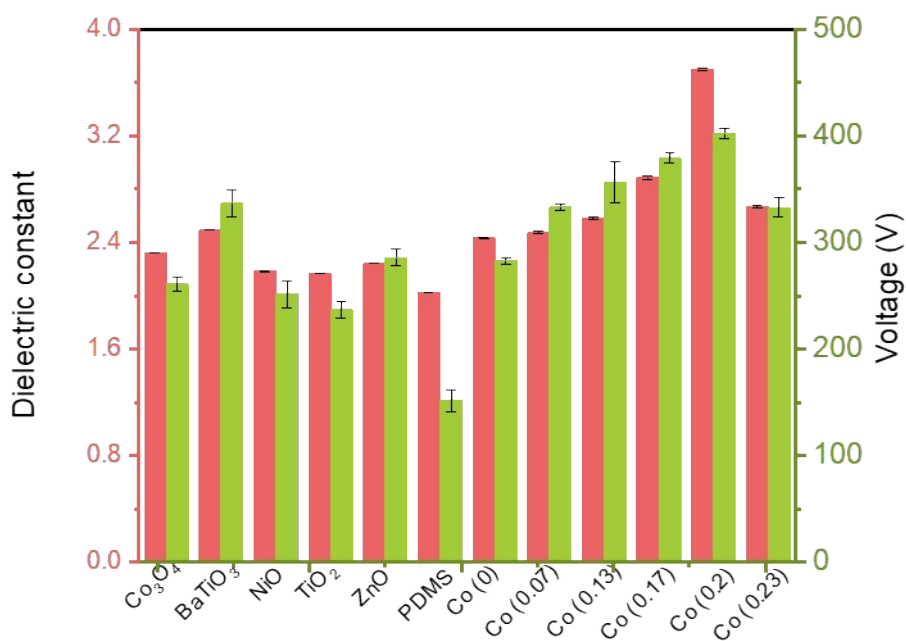


Fig. S7 Dielectric constants and voltages comparative plots of DEG with various materials used as intermediate layer.

Part 11:

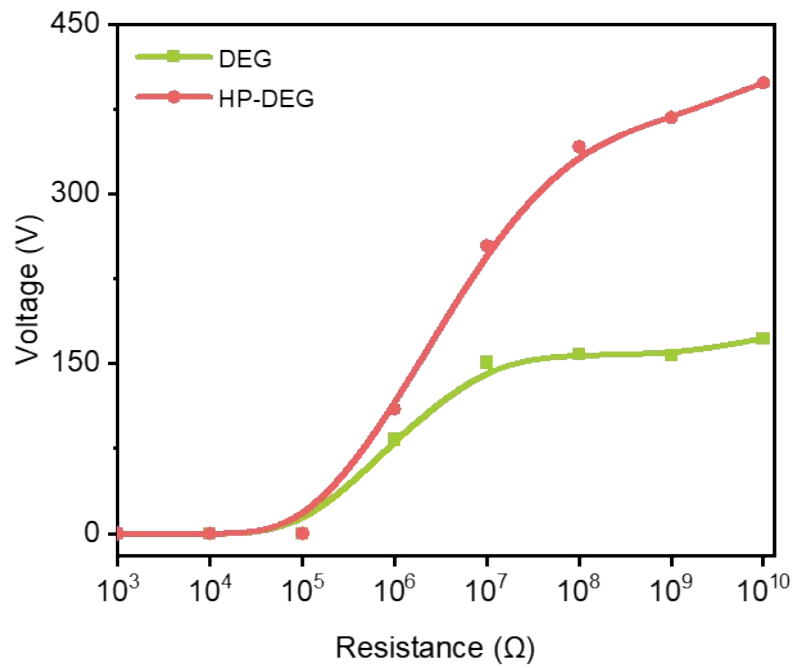


Fig. S8 Voltage output of DEG and HP-DEG with different load resistances.

Part 12:

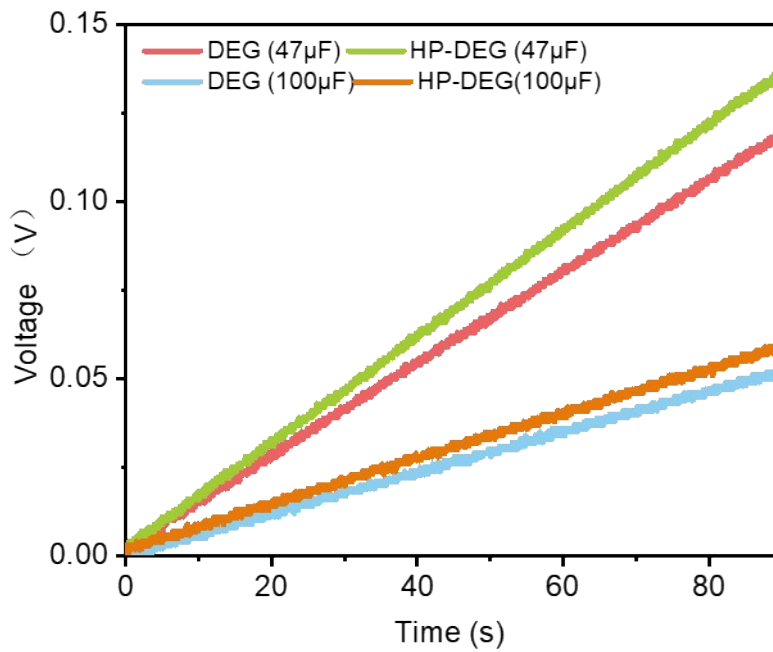


Fig. S9 Voltage output of DEG, HP-DEG by charging 47/100 μF capacitors.

Part 13:

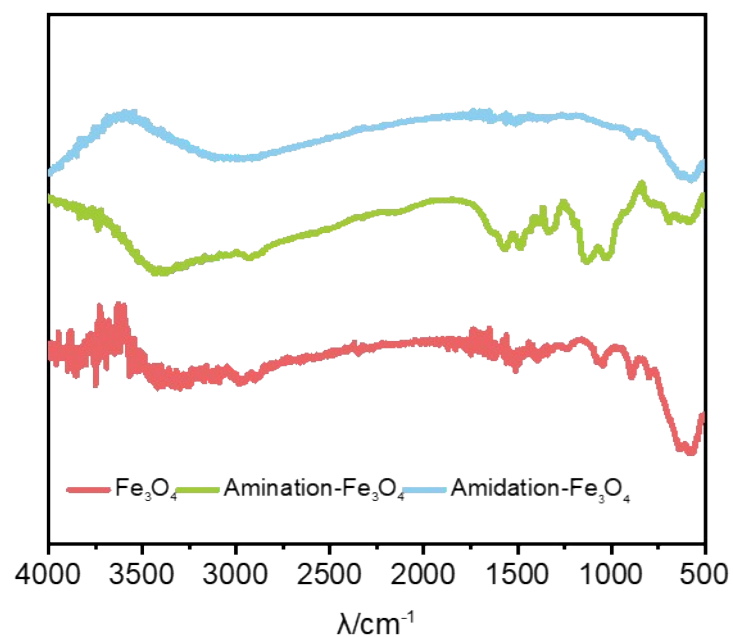


Fig. S10 FTIR spectroscopy of Fe_3O_4 , amido- Fe_3O_4 , amido- Fe_3O_4 modified on capture probe.

Part 14:

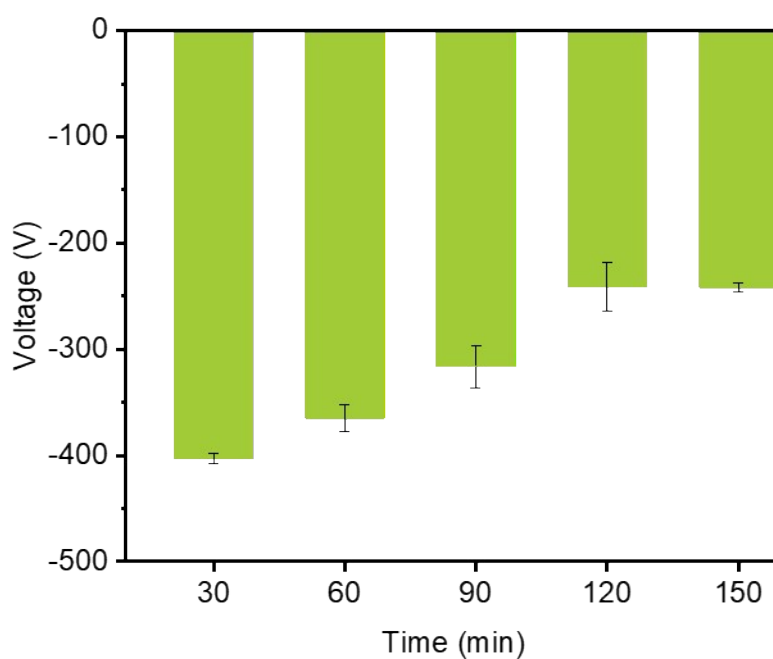


Fig. S11 Voltage output of HP-DEG for bacterial DNA sensing with different reaction times for DNA complex formation (30, 60, 90, 120, 150 min).

Part 15:

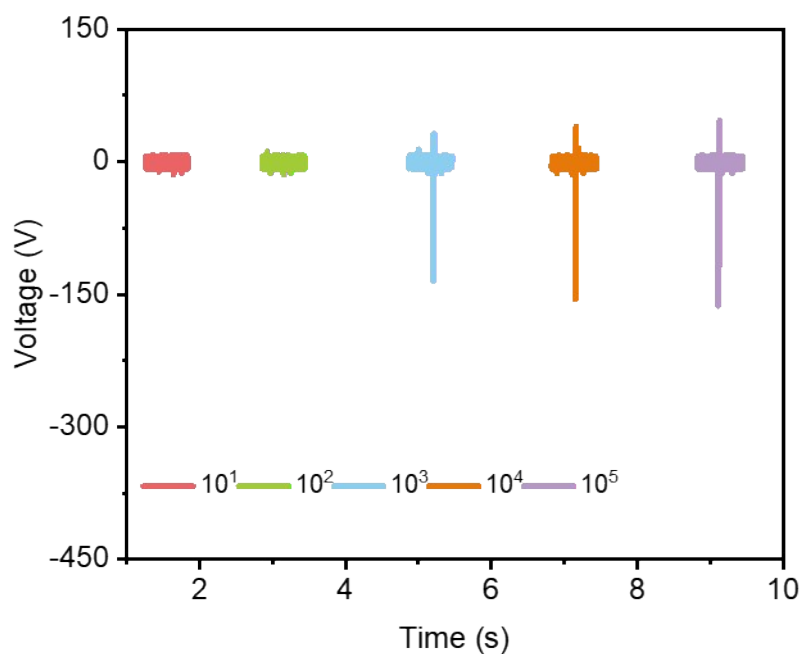


Fig. S12 Voltage output of DEG with different dilutions of CNTs. After taking 10 ml of the original solution, the dilutions were 10¹, 10², 10³, 10⁴, 10⁵ respectively.

Part 16:

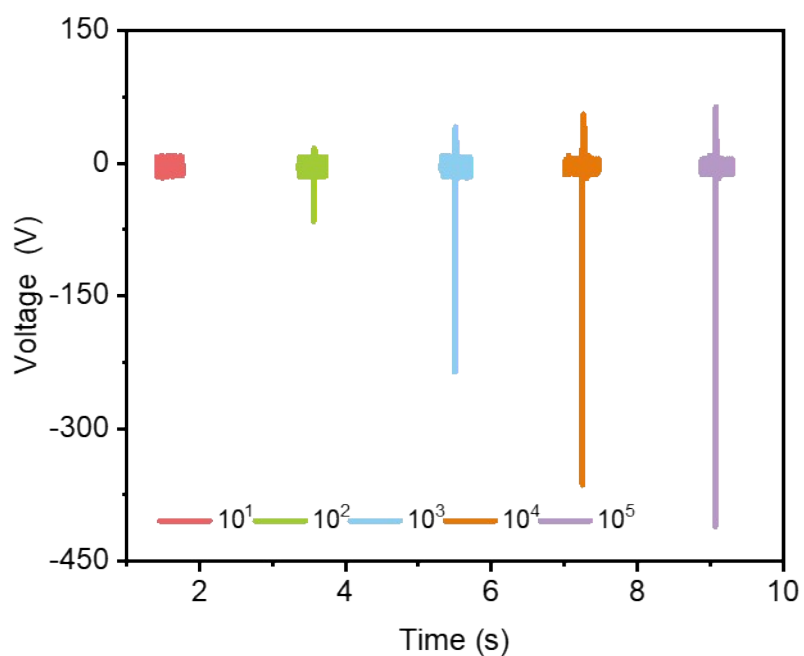


Fig. S13 Voltage output of HP-DEG with different dilutions of CNTs. After taking 10 ml of the original solution, the dilutions were 10¹, 10², 10³, 10⁴, 10⁵ respectively.

Part 17:

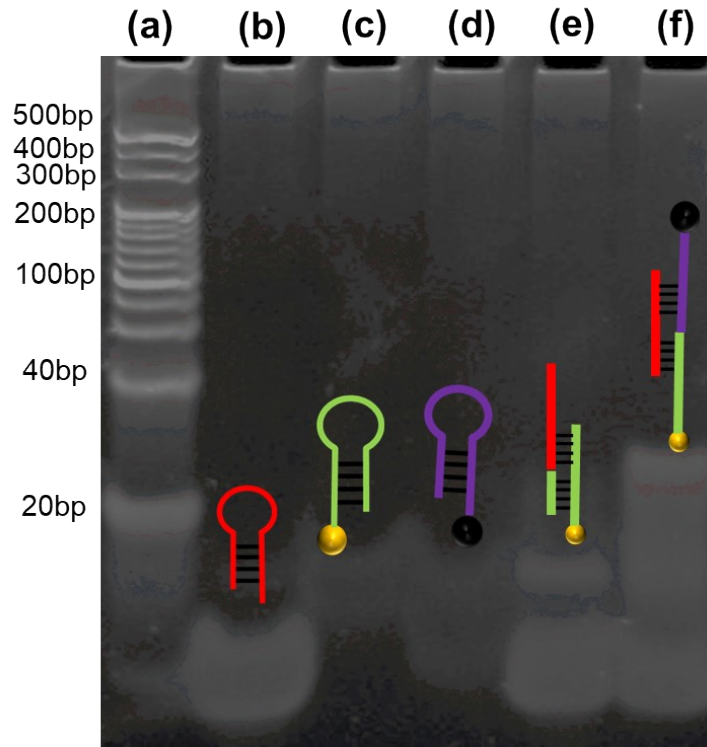


Fig. S14 DNA gel electrophoresis graph. (a) 20bp marker (b) DNA (c) Capture probe (d) Signal probe (e) Capture probe+DNA (f) Capture probe+DNA+Signal probe

Part 18:

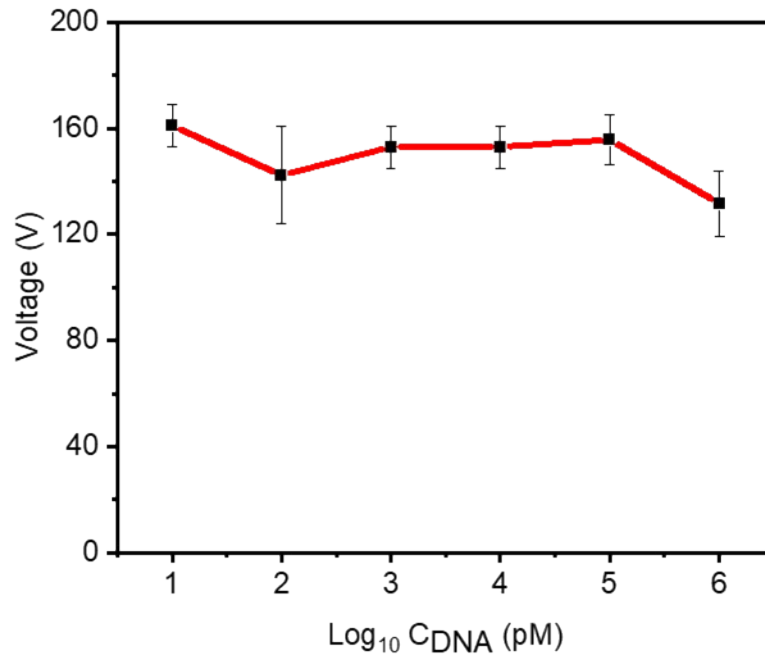


Fig. S15 Standard curve of DEG based bacterial DNA sensing.

Part 19:

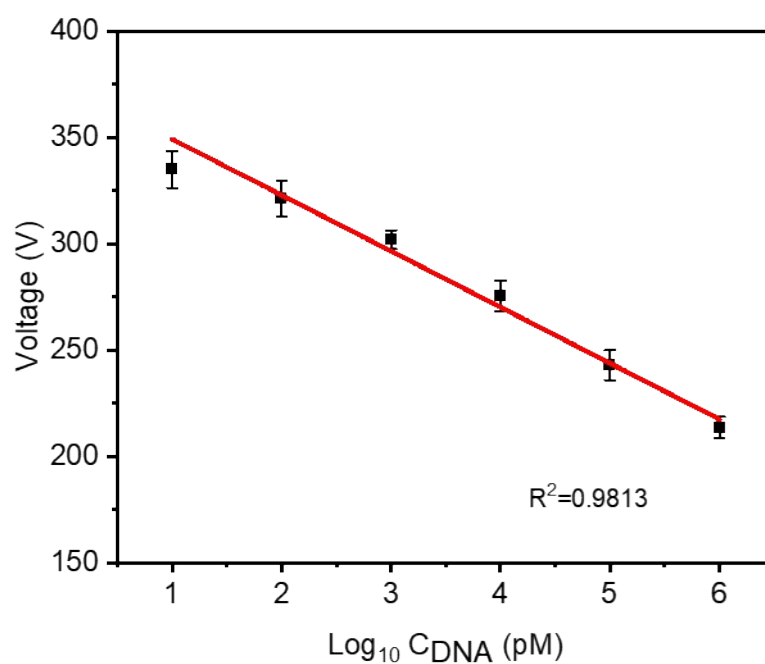


Fig. S16 Standard curve of HP-DEG based bacterial DNA sensing.

Part 20:

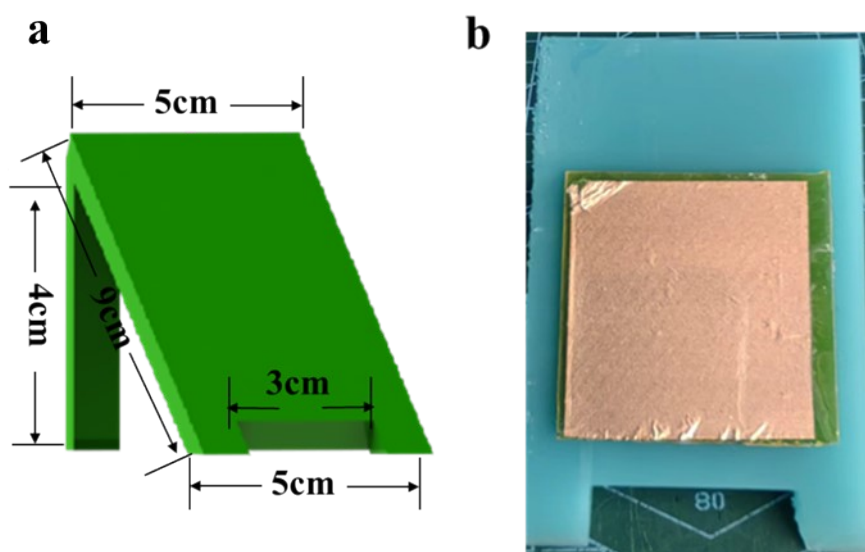


Fig. S17 HP-DEG based bacterial DNA sensing platform. a) 3D printed platform b) Physical specimen image.

References

- 1 Z. Xu, Z. Wang, D. Hu, H. Chen, Y. Yan, et al., *Advanced Functional Materials*, 2024, 2313118
- 2 Y. Deng, T. Zhou, K. Hu, Y. Peng, X. Jia, et al., *Biosensors and Bioelectronics*, 2024, **250**.
- 3 J. Shi, P. Li, Y. Huang, Y. Wu, J. Wu, et al., *Chemical Engineering Journal*, 2024, **483**.
- 4 F. Wang, C. Zhang, S. Deng, Y. Jiang, P. Zhang, et al., *Biosensors and Bioelectronics*, 2024, **252**.

5 T. Ye, Y. Xu, H. Chen, M. Yuan, H. Cao, et al., *Biosensors and Bioelectronics*, 2024, **251**.